ELSEVIER

Applied Catalysis B: Environmental 30 (2001) 75–85

APPLIED CATALYSIS B: ENVIRONMENTAL

www.elsevier.com/locate/apcatb

Redox behavior of CeO_2–ZrO_2 mixed oxides II. Influence of redox treatments on low surface area catalysts

H. Vidal [a,b], J. Kašpar [a,*], M. Pijolat [c], G. Colon [c,1], S. Bernal [b], A. Cordón [b], V. Perrichon [d], F. Fally [d,2]

[a] *Dipartimento di Scienze Chimiche, Università di Trieste, Via Giorgieri 1, Trieste 34127, Italy*
[b] *Departamento de Ciencia de los Materiales e Ingeniería Metalúrgica y Química Inorgánica, Universidad de Cádiz, Puerto Real 11510, Spain*
[c] *Ecole Nationale Supérieure des Mines, 158 Cours Fauriel, 42023 Saint Etienne Cedex-2, France*
[d] *Laboratoire d'Application de la Chimie à l'Environnement, UMR 5634, CNRS-Université, C. Bernard-Lyon 1, 43, Bd. Du 11 Novembre 1918, F 69622 Villeurbanne Cedex, France*

Received 21 May 2000; received in revised form 7 August 2000; accepted 7 August 2000

Abstract

Redox and textural/structural properties of low surface area (LS) ceria-zirconia mixed oxides with composition ranging from 0 to 85 mol% of ZrO_2, have been studied using Raman spectroscopy, X-ray diffraction, textural characterization, magnetic susceptibility measurements, temperature-programmed reduction and oxidation and buffering measurements. Special attention was given to the effects of aging under redox conditions. Correlation between chemical composition, textural, structural and redox properties of the oxides is reported. Comparison with previously reported high surface area (HS) samples shows that in spite of the initial low surface area of the present samples (≈20 versus ≈100 $m^2\,g^{-1}$), the reduction occurs at fairly low temperatures when zirconium is incorporated into the CeO_2 lattice. Remarkably, the favorable effects of the redox-aging on the reduction behavior are more pronounced in the present LS samples compared to the previously investigated HS ones. Raman and X-ray investigations revealed that important modifications of the structure take place as a consequence of the redox aging, leading to appreciable CeO_2 segregation, which could suggest some correlation between these parameters.

Keywords: CeO_2–ZrO_2 mixed oxides; Oxygen storage capacity (OSC); Oxygen buffering capacity (OBC); Magnetic susceptibility; Raman spectroscopy; X-ray diffraction; Structural and redox properties; Three-way catalysts

1. Introduction

Ceria-zirconia mixed oxides represent the state-of-art of the so-called oxygen storage capacity (OSC) in automotive exhaust catalysts [1]. Their ability to release/acquire oxygen through redox processes involving the Ce^{4+}/Ce^{3+} couple, i.e. OSC, provides a way to increase the efficiency of the three-way catalysts (TWCs) by enlarging the air-to-fuel window. Advent of the "light-off catalyst", i.e. a secondary converter close coupled to the engine, exposes TWCs to high temperatures, which requires for thermal stability of the OSC promoter. The introduction on the market of these mixed oxides was indeed motivated by their

* Corresponding author. Fax: +39-40-6763903.
E-mail address: kaspar@univ.trieste.it (J. Kašpar).
[1] On leave from Instituto de Ciencia de Materiales-CSIC, Avda, Americo Vespucio s/n, Isla de la Cartuja, 41092 Sevilla, Spain.
[2] On leave from Facultés Universitaires Notre-Dame de la Paix, Laboratoire LISE, Rue de Bruxelles 61, 5000 Namur, Belgium.

0926-3373/01/$ – see front matter
PII: S0926-3373(00)00221-6

high thermal resistance [2–6]. In the preceding paper we investigated the redox behavior and the effects of redox-aging of a series of ceria-zirconia mixed oxides with high surface area (approximately 100 m^2/g) and CeO_2 content ranging from 15 to 100 mol% [7]. Here, a parallel study carried out on low surface area (LS) samples prepared by thermal aging at 1173 K [8] is reported. In fact, thermal stability of the TWCs is an important topic in view of Euro phase IV and recent US Tier 2 proposals which require a high durability (up to 120,000 miles) of the TWCs and installation of on-board diagnostics (OBD) in gasoline-engine vehicles. OBD monitors the efficiency of the OSC using an oxygen sensor. Loss of OSC is taken as an indication of a deactivated catalyst, which points out the necessity of thermal stability of redox properties. Thermal aging of traditional CeO_2-based TWCs typically leads to loss of both surface area and OSC, the latter being detected by loss of reduction at low temperatures [9,10]. Accordingly the present study addresses the redox properties of LS CeO_2–ZrO_2 mixed oxides, which were prepared from HS samples by subjecting to a thermal treatment to obtain a partial sintering of the mixed oxides [8].

2. Experimental

The CEZIRENCAT [3] oxides here employed were synthesized by Rhodia. A detailed characterization is reported in [8]. Hereafter they will be referred to as CZ-XX/YY-LS, where "LS" indicates that the oxide has a low surface area (approximately 20–30 $m^2\,g^{-1}$), and "XX/YY" indicates its Ce/Zr molar ratio composition (15/85, 50/50, 68/32, 80/20 and 100/0). These oxides were prepared from the corresponding HS samples by calcination in air at 1173 K for 140 h in the presence of water.

The details of the experimental techniques here employed are reported in part I [7]. The following techniques were employed: temperature programmed reduction and oxidation (TPR and TPO); the oxygen storage as measured by magnetic susceptibility, O_2 uptake and oxygen buffering capacity (OBC) measurements; textural and structural properties were studied, respectively, by N_2 adsorption at 77 K, powder X-ray diffraction and Raman spectroscopy. The following reduction/oxidation procedure was typically applied to the catalysts in order to investigate the effects of the redox-aging. After the standard cleaning pre-treatment in O_2 (5%)/Ar at 823 K for 1 h, the reduction was carried out in a flow of 25 ml min^{-1} of H_2 (5%)/Ar from room temperature (RT) to 1273 K at a heating rate of 10 K min^{-1}. Then the sample was held at this temperature for 15 min. The flow was switched to Ar and after 15 min at 1273 K the sample was cooled slowly down to 700 K (or to RT in the case of the TPO experiments). At this point the sample was re-oxidized by pulsing O_2 (0.125 ml) every 75 s. To investigate the effects of redox-aging each reducing/oxidizing sequence was performed three times. A sample obtained from such a treatment will be hereafter indicated as "redox-aged". Specific redox-aged samples were prepared also for the magnetic susceptibility, XRD and textural studies. In these cases the maximum reduction temperature was 1223 K.

[3] The CEZIRENCAT is a multi-laboratory project in the area of three-way catalysis funded by the European Union. Home page: http://www.dsch.univ.trieste.it/cezirencat.

3. Results and discussion

3.1. Textural study

Results of textural characterization of the starting and redox-aged LS CeO_2–ZrO_2 mixed oxides are summarized in Table 1. Thermal aging applied for the preparation of the LS samples leads to similar textural properties for all the LS samples, with exception of the CZ-15/85-LS sample which has a significantly higher BET surface area compared to other samples. Redox-aging hardly affected the surface area and pore volume in all samples, indicating that full extent of textural modification have been induced by the prior thermal treatment. As shown by the V_{micro} values, all the samples are essentially mesoporous, the cumulative pore volume being about one-half/one-third of that of HS samples. A good thermal stability under reducing conditions is of interest in view of previous observation that such conditions strongly promoted sintering of CeO_2 [11].

Table 1
Textural properties of the LS oxides

Sample	Number of cycles	S_{BET} ($m^2\,g^{-1}$)	S_t[a] ($m^2\,g^{-1}$)	Cumulative pore volume ($cm^3\,g^{-1}$)	V_{micro} ($cm^3\,g^{-1}$)	Average pore diameter (nm)
CZ-100/0-LS	0	20	17	0.162	0.0005	11.5
CZ-80/20-LS	0	15	14	0.118	0.0000	25
	1	15	13	0.111	0.0003	25
	3	13	12	0.135	0.0001	30
CZ-68/32-LS	0	23	15	0.167	0.0031	22
	1	21	15	0.184	0.0024	22
	3	20	18	0.185	0.0004	22.5
CZ-50/50-LS	0	21	17	0.134	0.0011	25
	1	18	16	0.138	0.0007	22
	3	17	13	0.131	0.0015	22.5
CZ-15/85-LS	0	30	28	0.208	0.0019	22

[a] Surface area measured from t-plot.

3.2. Temperature-programmed reduction, oxygen storage and oxygen buffering experiments

3.2.1. Temperature programmed reduction

Fig. 1 shows the TPR profiles of the as-prepared LS oxides (indicated as TPR1) and the effects of TPR/oxidation treatments (indicated as TPR2 and TPR3, respectively, for second and third TPR, each carried out after re-oxidation at 700 K). Despite a five-fold decrease of surface area in the LS samples with respect to the HS ones, similar reduction features are found since a single main reduction feature is observed around 850 K in both types of samples. This is a remarkable observation and it points out that despite the thermal aging the favorable redox properties of CeO_2–ZrO_2 mixed oxides are preserved since reduction at low temperature is still present. In fact, the reduction profiles obtained for CeO_2 (not shown) presented a single reduction peak at 1100 K, indicating loss of low-temperature redox properties [9,12].

A comparison of the TPR profiles of the fresh LS samples with those reported in the previous paper [7] shows that the initial thermal aging induces, however, significant changes of the reduction behavior. In fact, all the profiles of the LS samples are still characterized by a single major reduction feature, which, except for CeO_2 shifts to higher temperatures with increasing ZrO_2 content, however, the additional reduction features, e.g. the broad reduction peak at 900–1273 K, are now rather intense, particularly in the CZ-80/20-LS sample. There is also a general increase of the peak temperatures by about 15–30 K for the LS mixed oxides compared to the HS ones, suggesting that an initial high surface area facilitates the reduction process.

As far as the effects of the redox-aging are concerned, the general appearance follows that reported for the HS samples, e.g. under the present experimental conditions the redox aging improves the reducibility of the mixed oxides at low temperatures and major changes are observed after the first redox cycle. Further redox-aging affects the TPR profile to a very minor extent (compare Fig. 1, TPR2 and TPR3 curves and Table 2). However, the response of the system is sometimes different with respect to the HS samples. For example, only a small shoulder at the low temperature end of the main reduction peak was generated by redox aging in the CZ-80/20-HS sample, which becomes a strong peak at about 650 K in the corresponding LS sample. The opposite is observed in the CZ-50/50-LS sample, which is slightly modified by the redox procedure, while the corresponding HS sample was strongly modified. When comparing the TPR behavior of the CZ-15/85-HS and LS samples, it should be borne in mind that some non-incorporated *m*-ZrO_2, detected in the former sample, was incorporated into a solid solution upon the thermal aging leading to the LS oxide [8]. An interesting observation is that the main peak, which is present in the initial TPR, is almost unaffected by the

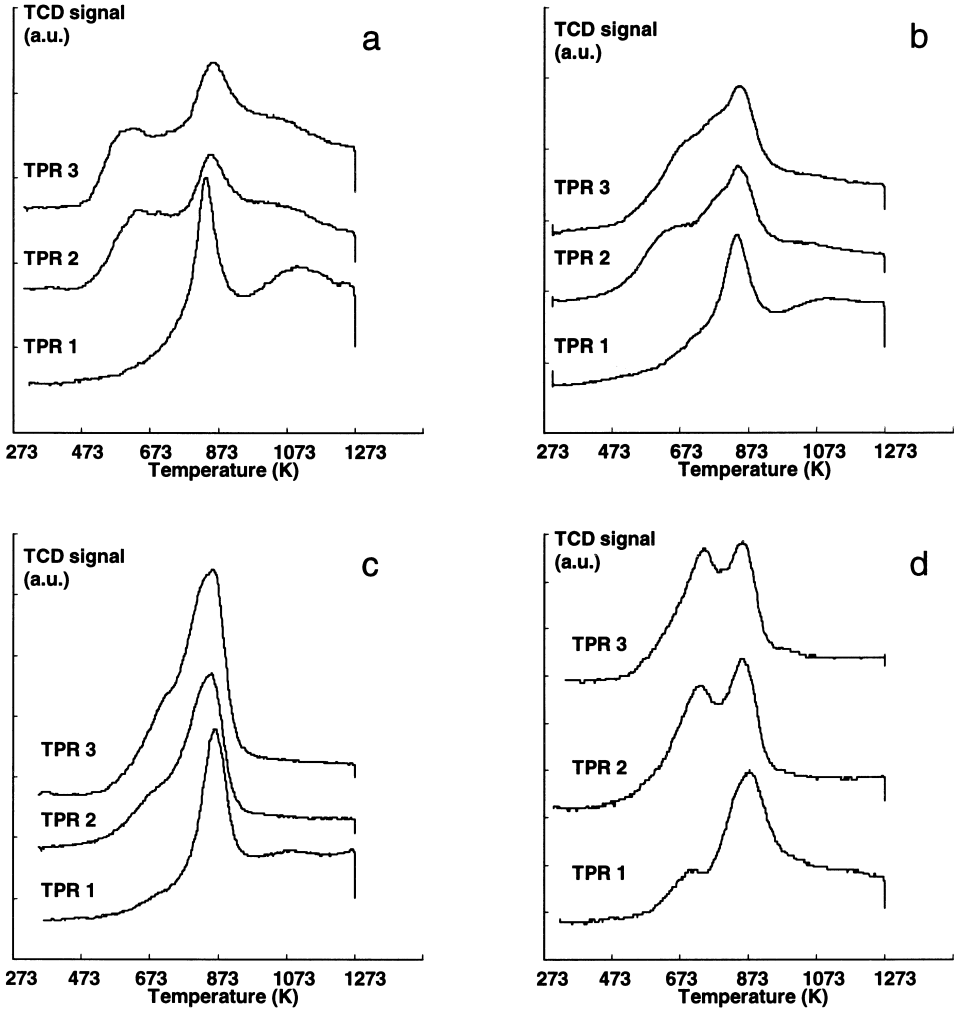

Fig. 1. Effect of redox cycling on the TPR profiles of (a) CZ-80/20-LS, (b) CZ-68/32-LS, (c) CZ-50/50-LS and (d) CZ-15/85-LS. TPR1: fresh sample, TPR2 and TPR3: sample recycled from, respectively, run TPR1 and TPR2.

composition of the mixed oxide, while the position of the low temperature peak, which is generated by redox-aging, moves down with increasing Ce content (Table 2). In summary, thermal aging modifies the TPR behavior of the LS samples with respect to HS ones as the reduction occurs at higher temperatures. This undesirable effect is compensated by the effects of redox-aging, since after this treatment the reduction occurs at fairly low temperatures, which are even lower that those observed in corresponding redox-aged HS samples.

3.2.2. OSC and TPO measurements

After each TPR experiment, samples were re-oxidized by O_2 pulses at 700 K and the O_2 uptake was measured. Table 2 summarizes the measured OSC.

Redox-aging does not affect the total OSC, except for CZ-50/50-LS where a small but significant increase of OSC with redox-cycles is observed. Fig. 2 shows that the percentage of Ce^{3+} formed during the reduction process of the samples (estimated from the OSC experiments) increases with the Zr content. In the case of the HS oxides, this was attributed to the fact that a

Table 2
TPR peak temperatures and O_2 uptakes measured at 700 K over the LS CEZIRENCAT oxides: effects of TPR/oxidation cycles

Sample	Number of cycles	Peak maximum (K)	O_2 uptake (mmol g^{-1})[a]	Ce^{3+} (%)[b]
CZ-100/0-LS	0	1160[c]	0.58	40
	1	1130	0.58	40
	2	1130	0.55	38
CZ-80/20-LS	0	840	0.69	56
	1	650, 860	0.68	56
	2	635, 865	0.70	57
CZ-68/32-LS	0	845	0.72	66
	1	685, 850	0.71	65
	2	705, 855	0.72	66
CZ-50/50-LS	0	865	0.62	73
	1	715, 850	0.65	77
	2	740, 855	0.66	78
CZ-15/85-LS	0	720, 880	0.25	87
	1	735, 860	0.24	84
	2	745, 860	0.25	86

[a] S.D. $\pm$ 0.01 mmol g^{-1}.
[b] Estimated from the O_2 uptake, assuming a full re-oxidation of the sample.
[c] A very small peak was also detected at 755 K, which could be attributed to reduction of surface and/or residual surface impurities.

constant composition of $Ce_mZr_{1-m}O_{1.78}$ was attained after reduction at 1273 K for all the mixed oxides, except CZ-85/15-HS [7]. Here, the oxygen stoichiometry varies with the zirconium content, indicating that generation of the reduced oxides is affected by the origin of the sample, e.g. HS or LS. A maximum degree of reduction is observed for the CZ-68/32-LS oxide ($Ce_{0.68}Zr_{0.32}O_{1.77}$), which is similar to the composition obtained with the HS sample.

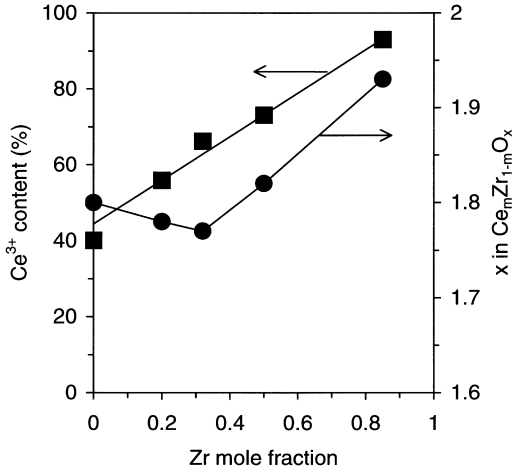

Fig. 2. Cerium reducibility as a function of the zirconium content, estimated from the O_2 uptake measurements at 700 K after a reduction at 1273 K.

The re-oxidation process was investigated by pulsing O_2 over the catalysts at 700 K and also by TPO experiments. Fig. 3 reports the cumulative O_2 uptake during the pulse experiments performed at 700 K over the LS samples. A perusal of Fig. 3 reveals that the re-oxidation of CZ-68/32-LS and CZ-80/20-LS is more difficult compared to CZ-15/85-LS, CZ-50/50-LS and CZ-100/0-LS. For the latter group the curve steadily and almost linearly increases up to over 90% of the full uptake, indicating a very fast and effective re-oxidation of the mixed oxides, which proceeds effectively even in the bulk. We recall that the samples have been reduced at 1273 K before the experiment. Differently, the immediate deviation from linearity observed for the CZ-68/32-LS and CZ-80/20-LS samples is an indication of a partial uptake of the O_2 pulse, suggesting that re-oxidation kinetics are relatively slow compared to the residence time of the O_2 pulse ($\leq$0.04 s). These results are consistent with those observed on HS samples, however, it should be noted that an overall loss of efficiency of

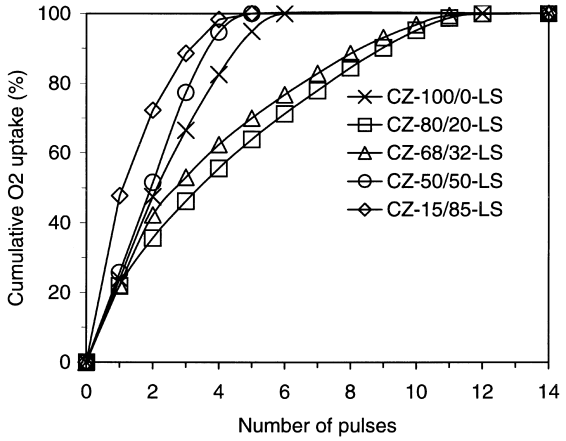

Fig. 3. Cumulative O_2 uptake obtained in the re-oxidation at 700 K of CZ mixed oxides reduced at 1273 K: (×) CZ-100/0-LS, (□) CZ-80/20-LS, (△) CZ-68/32-LS, (○) CZ-50/50-LS and (◇) CZ-15/85-LS.

the re-oxidation process is observed here since under identical experimental conditions the re-oxidation was completed within eight pulses for all the HS samples [7].

As shown in Fig. 4, which reports the TPO experiments, the re-oxidation takes place in two steps; the first one, which accounts up to 75% of the overall uptake, occurs at RT. Its shape somewhat changes with composition, and it is rather broad and tailing in CZ-68/32-LS and CZ-80/20-LS, indicating a slower re-oxidation. The second peak is centered around 373 K and it represents a thermally activated re-oxidation process. It is more intense for the CZ-68/32-LS and CZ-80/20-LS compositions. No detectable modification of the re-oxidation process has been detected upon redox-aging.

3.2.3. OBC experiments

Oxygen storage under kinetic control was measured using the OBC technique [13] (Table 3). In this method O_2 is pulsed over the sample in a flow of inert gas to analyze the ability of the oxide to attenuate fast oscillations in O_2 partial pressure. Though not included, pure CeO_2, i.e. CZ-100/0-LS, did not exhibit any OBC. This is consistent with the observation that in this oxide oxygen storage is associated with surface processes only [9].

As it can be noted in Table 3, the higher the temperature, the higher the ability of the oxides to attenuate fast oscillations in the O_2 signal. However, the most significant result is the increase of the

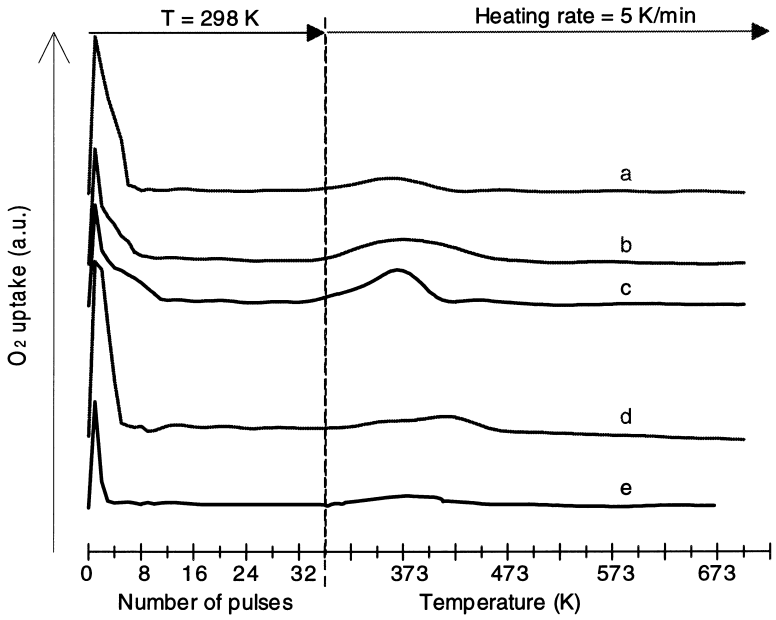

Fig. 4. TPO profiles of CZ mixed oxides reduced at 1273 K: (a) CZ-100/0-LS, (b) CZ-80/20-LS, (c) CZ-68/32-LS, (d) CZ-50/50-LS and (e) CZ-15/85-LS.

Table 3
OBC (%) of the LS oxides as a function of the redox cycling and temperature

Sample	Number of cycles	673 K	923 K	1173 K
CZ-80/20-LS	0	4	24	75
	1	7	27	73
	3	9	24	75
CZ-68/32-LS	0	1	21	69
	1	4	34	79
	3	6	33	81
CZ-50/50-LS	0	0	15	65
	1	7	32	74
	3	5	36	81

OBC as consequence of redox-aging, particularly for the Zr-rich oxides. Although initially low, following the redox-aging the OBC reaches the levels attained by the HS sample with same composition [7]. This indicates that redox-aging has a favorable effect which can compensate for the strong worsening of the textural properties on passing from HS to LS samples. This is consistent with the TPR results and those derived from the magnetic susceptibility measurements (see below).

3.3. Magnetic susceptibility measurements

Fig. 5 represents the reduction percentages as a function of temperature calculated for the LS and HS samples from the magnetic balance experiments. These results show that CZ-80/20-LS, CZ-68/32-LS and CZ-50/50-LS show similar percentage of Ce^{3+} up to 700 K. Above this temperature cerium reducibility grows with zirconia content. On the other hand, CZ-15/85-LS exhibits the highest reduction percentage among the low surface area oxides. The comparison of these results with those previously reported for the HS oxides shows that high surface area generally favors cerium reducibility in the fresh samples.

The effects of redox-aging as investigated by magnetic measurements are in a very good agreement with the TPR results above commented. As shown in Fig. 6a, in which CZ-50/50-LS was selected as a representative of the whole series, cerium reducibility is improved upon redox-aging. Compared to the initial LS sample, the improvement in the reduction percentage is already observed after one redox cycle (Fig. 6b).

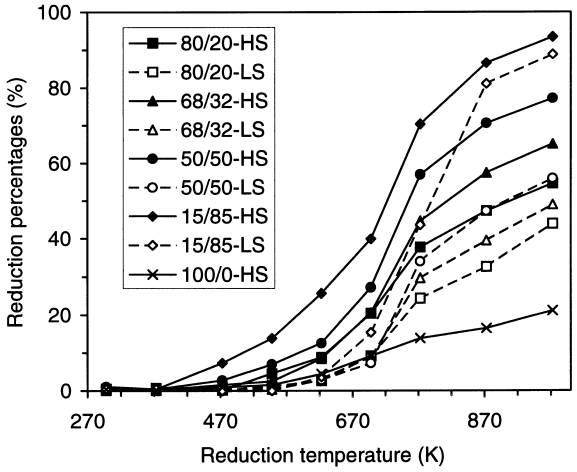

Fig. 5. Effects of texture on the reduction percentage estimated from the magnetic susceptibility measurements as a function of reduction temperature (1 h at each temperature).

The improvement of the reducibility induced by the three redox-aging cycles performed on CZ-50/50-LS is remarkable, showing a maximum improvement at 700 K of about 45% in comparison to the starting sample. In the three times redox-aged LS sample the content of Ce^{3+} above 700 K has become almost the same as or even higher than that of CZ-50/50-HS, thus attenuating the differences ascribable to the initial texture.

Finally, we have also studied the re-oxidation of the LS samples by introducing small doses of pure O_2 in a similar way to that applied over the high surface area oxides. For comparison, some data obtained on HS oxides and some recycled samples have been included in Table 4. The most significant conclusion from this study is that while for the HS samples re-oxidation is almost completed at RT, for the LS and recycled oxides it is necessary to heat them to achieve full oxidation. This result fits well with above discussed observations from TPO and O_2 uptake at 700 K experiments, which indicated a slower kinetic for the re-oxidation of the low surface area samples, especially for CZ-68/32-LS and CZ-80/20-LS.

3.4. Structural characterization

3.4.1. FT Raman spectroscopy

Raman spectra of fresh and redox-aged LS samples are reported in Fig. 7. Six Raman-active modes

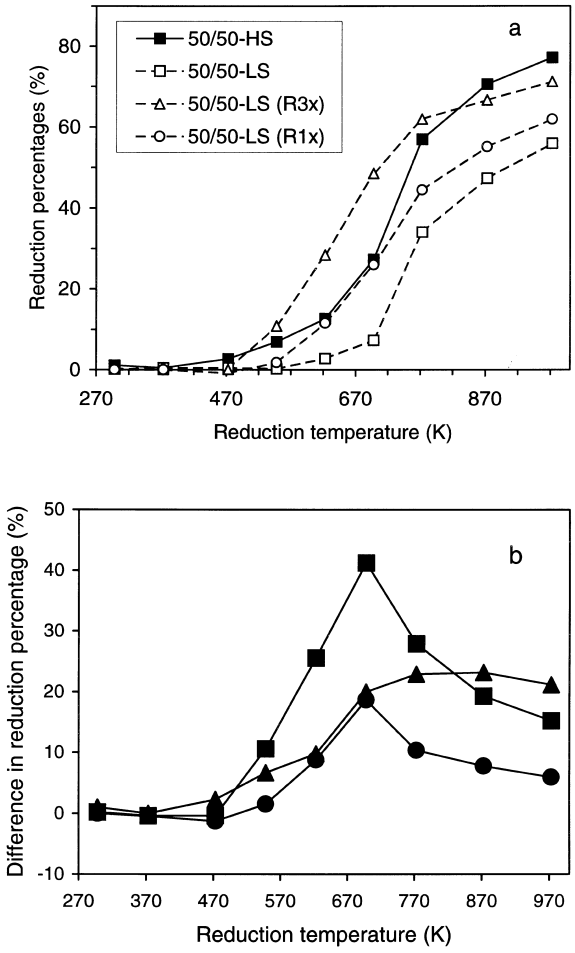

Fig. 6. Effect of redox-aging on the reduction percentage estimated from magnetic susceptibility for CZ-50/50-LS (a) (R1×/R3×: redox-aged once/three times), the improvement in the reduction percentage induced by redox-aging and the comparison with CZ-50/50-HS with respect to the CZ-50/50-LS (b): (■) redox-aged three-times — LS; (●) redox-aged once — LS and (▲) difference HS − LS.

of the $A_{1g} + 3E_g + 2B_{1g}$ symmetry are predicted for tetragonal ZrO_2 (space group $P4_2/nmc$), while for the space group *Fm*3*m* (fluorite lattice) only one F_{2g} mode centered at around 490 cm^{-1} is Raman-active [13]. This mode is observed at 465 cm^{-1} in CeO_2. No modification of the Raman spectrum is detected in the CZ-100/0-LS sample (data not reported), which spectrum is characterized by a single peak centered at 465 cm^{-1} of F_{2g} symmetry.

Consistently with presence of a solid solution, this peak is shifted to 472 cm^{-1} in the case of CZ-80/20-LS, and is largely unaffected by the redox-aging excepting a slight shift towards higher frequencies. Also, the Raman spectrum of CZ-15/85-HS is hardly affected by the redox-aging, since the six Raman bands of the tetragonal (t) phase are detected in both spectra. Notice, however, that partial CeO_2 segregation would have escaped to detection due to the overlap of the band at 463 cm^{-1} with the F_{2g} mode of CeO_2.

In contrast, significant modifications of the Raman spectra are detected in both CZ-68/32-LS and CZ-50/50-HS. A new strong peak at 464 cm^{-1} is detected in the former sample (Fig. 7b) suggesting some ceria segregation (see below). The Raman spectrum of fresh CZ-50/50-LS was assigned to a tetragonal (t″) phase and it is characterized by an intense peak at 473 cm^{-1} and weak bands at 305 and 136 cm^{-1} [8]. Remarkably, even the intense feature at 473 cm^{-1} almost disappears upon redox-aging, suggesting that an important modification of the oxygen sublattice occurred (Fig. 7c). On the other hand, a very small peak at 464 cm^{-1} tentatively attributed to ceria segregation is observed in the spectrum of the redox-aged sample. However, its low intensity denotes less importance of this phenomenon compared to the CZ-68/32-LS.

3.4.2. X-ray diffraction

Powder XRD patterns were collected on fresh and redox-aged samples. As shown in Fig. 8, for two representative compositions, e.g. CZ-68/32-LS and CZ-50/50-LS, after redox-aging the main peak ((1 1 1) in the corresponding solid solution) is rather broad and asymmetric. This suggests that the redox treatment affects the structure of the oxide, as indicated by the appearance of shoulders on both sides of the peak, one of them corresponding to CeO_2. We recall that some phase segregation upon redox-aging was also detected in the HS samples, however to a smaller extent (<5%). Also to be noticed that improvement of redox properties was also found already after the first redox cycle (Fig. 1).

The effects of redox aging on CZ-68/32-LS were analyzed in some detail (Table 5). The sample was reduced at the indicated temperatures for 1 h and then oxidized at 700 K. An almost constant cell para-

Table 4
Residual Ce^{3+} percentages (%) after oxidation under oxygen (40 Torr) at 298 K and after heating at 823 K

Samples	Ce^{3+} (%)					
	HS			LS		
	Under O_2 at 298 K	After 823 K under O_2	$(\Delta Ce^{3+})^a$	Under O_2 at 298 K	After 823 K under O_2	$(\Delta Ce^{3+})^a$
Fresh						
CZ-80/20	1.3	0.8	−0.5	1.9	1.1	−0.8
CZ-68/32	1.5	0.7	−0.8	5.2	1.1	−4.1
CZ-50/50	2.2	1.7	−0.5	9.9	2.6	−7.3
CZ-15/85	0.1	0.0	−0.1	4.2	0.0	−4.2
Redox-aged						
CZ-68/32-(R3x)	6.1	1.5	−4.6	3.3	1.4	−1.9
CZ-50/50-(R3x)	5.0	1.7	−3.3	2.6	0.8	−1.8

[a] Variation of Ce^{3+} percentages after heating treatment at 823 K under O_2 (40 Torr).

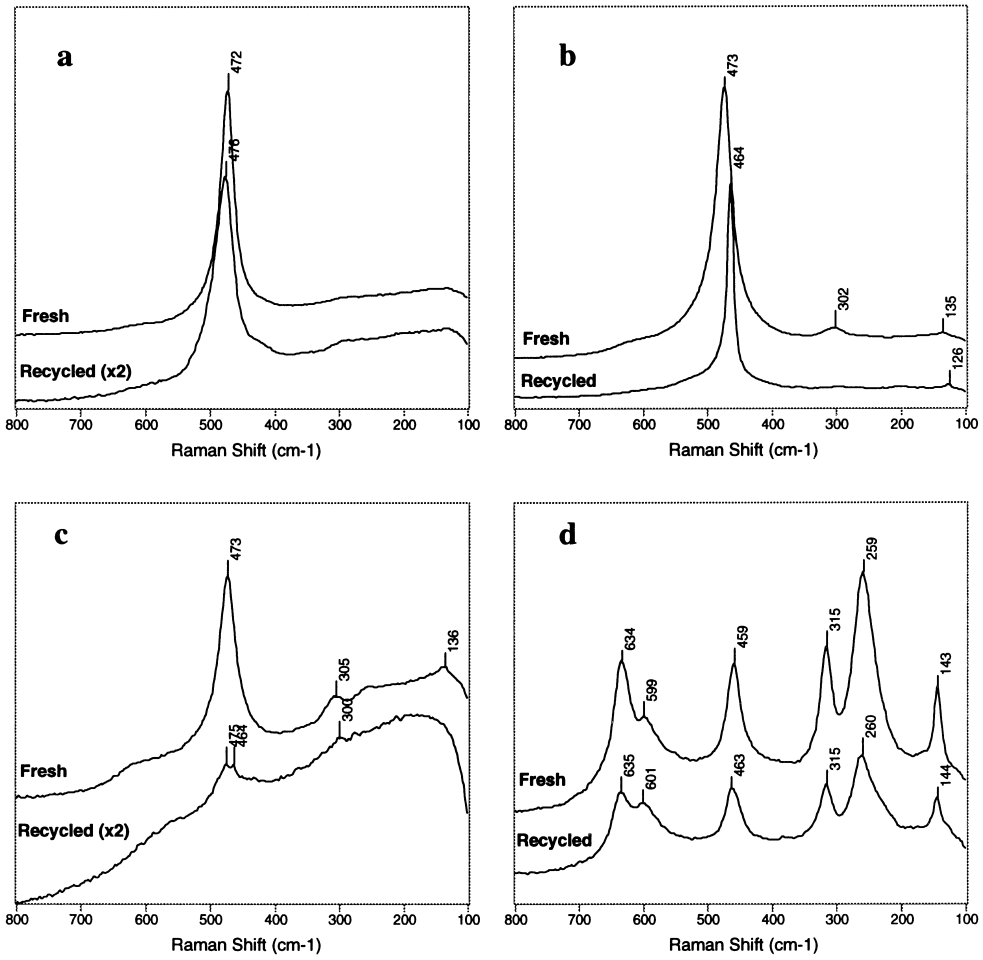

Fig. 7. Effects of redox-aging on the Raman spectra of CZ-80/20-LS (a), CZ-68/32-LS (b), CZ-50/50-LS (c) and CZ-15/85-LS (d). Spectra were multiplied by the factor reported in parentheses.

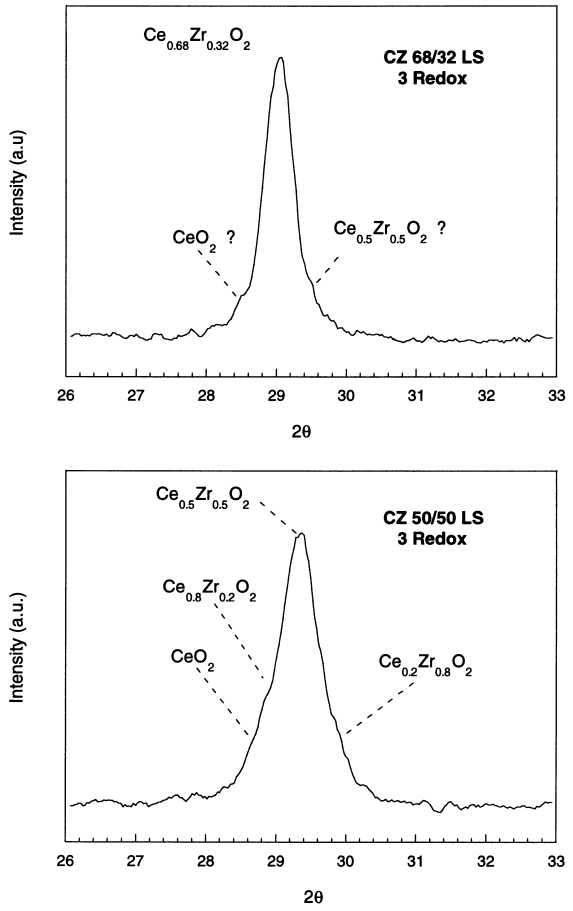

Fig. 8. X-ray diffraction patterns of CZ-68/32-LS and CZ-50/50-LS samples redox-aged for three redox-cycles.

meter and no evidence of sample non-homogeneity is observed for treatments up to 1173 K. In contrast, reduction at 1273 K, followed by oxidation at 700 K, leads to segregation of detectable amounts of CeO_2 from the mixed oxide. Further redox-aging increases the amount of segregated CeO_2 with a corresponding decrease of lattice parameter, as expected for a phase being enriched in Zr. The comparison of these results with the Raman spectra is of interest, since it indicates a good sensitivity of the Raman technique in detecting even small amounts of segregated CeO_2. At present a direct correlation between CeO_2 segregation and favorable redox properties as induced by redox-aging cannot be discerned. However, it should be noticed that except the CZ-80/20 samples, direct evidence for CeO_2 segregation upon aging or compositional inhomogeneity (CZ-15/85) has always been detected. Noticeably, the favorable effects of the high temperature reduction followed by a mild oxidation were previously reported for a $Ce_{0.5}Zr_{0.5}O_2$ mixed oxide containing significant amounts of non-incorporated CeO_2 [10]. Evidence for favorable effects of a domain type of structure of CeO_2–ZrO_2 mixed oxides on the reduction behavior was also reported [14].

4. Conclusions

This study has shown that ceria–zirconia system presents good redox properties and high OSC even when pre-sintered by a high temperature calcination. In addition, redox-aging further improves the reducibility, OSC and OBC properties of the pre-sintered oxides. This behavior is consistent with that observed over the HS samples, however, the degree of promotion is higher in the case of LS samples.

The most relevant observations derived from the study performed over the LS samples are summarized as follows:

Table 5
Effects of redox treatments on CZ-68/32-LS as detected from powder XRD patterns

Treatment	Cell parameter[a]	Particle size (nm)	Phase (space group)
Fresh sample	5.3454 ± 0.0009	15.0	Cubic (*Fm*3*m*)
Reduction at 773 K for 1 h	5.3447 ± 0.0011	14.0	Cubic (*Fm*3*m*)
Reduction at 973 K for 1 h	5.3442 ± 0.0018	14.0	Cubic (*Fm*3*m*)
Reduction at 1173 K for 1 h	5.3398 ± 0.0006	15.6	Cubic (*Fm*3*m*)
One redox cycle[a]	5.3253 ± 0.0009	17.6	Cubic (*Fm*3m) + CeO_2 (<5%)
Three redox cycles[a]	5.3221 ± 0.0020	17.5	Cubic (*Fm*3*m*) + CeO_2 (≈10%)[b]

[a] Reduction up to 1273 K in each cycle.
[b] Particle size (>100 nm).

- Mixed oxides are reduced at much lower temperatures than pure ceria through a process which appears to occur concurrently on the surface and in the bulk. This positively affects both OSC and OBC.
- This effect is enhanced slightly with ceria content and is clearly improved upon redox-aging.
- The study of the re-oxidation process, both by TPO and O_2 uptake at 700 K, indicates that the rate changes with composition and it is faster for the Zr-richer samples. Most of the process already takes place at RT, and it is complete at approximately 373 K.
- Though the percentage of Ce^{3+} increases with Zr content, total OSC after reduction at 1273 K is higher for the mixed oxides with intermediate compositions, especially CZ-68/32-LS.
- Structural characterization evidences the occurrence of structural changes upon redox-aging, which nature depends on the chemical composition of the mixed oxide: small or no modifications are detected in both Zr- and Ce-rich samples, while for intermediate compositions the phase nature is strongly affected. Appreciable phase segregation occurs, which apparently have been favored by the pre-sintering of the mixed oxide.

Acknowledgements

The present study has received financial support from the TMR Program of the European Commission (Contract FMRX-CT-96-0060(DG12-BIUO)). H. Vidal, G. Colon and F. Fally acknowledge their fellowships from the TMR Program. The authors also thank Dr. R.T. Baker from Depto. de Ciencia de los Materiales e Ingeniería Metalúrgica y Química Inorgánica of University of Cadiz (Spain) for preparing the recycled samples that have been used for the magnetic susceptibility, XRD and textural studies. They also express their gratitude to Dr. R. Di Monte from Dipartimento di Scienze Chimiche of University of Trieste (Italy) for the analysis of the X-ray diffraction data.

References

[1] J. Kašpar, P. Fornasiero, M. Graziani, Catal. Today 50 (1999) 285, and references therein.
[2] L.L. Murrell, S.J. Tauster, D.R. Anderson, in: A. Crucg (Ed.), Catalysis and Automotive Pollution Control II, Stud. Surf. Sci. Catal., Vol. 71, Elsevier, Amsterdam, 1991, pp. 275–289.
[3] A. Trovarelli, C. de Leitenburg, G. Dolcetti, CHEMTECH 27 (1997) 32.
[4] T. Murota, T. Hasegawa, S. Aozasa, H. Matsui, M. Motoyama, J. Alloys Comp. 193 (1993) 298.
[5] G. Ranga Rao, J. Kašpar, R. Di Monte, S. Meriani, M. Graziani, Catal. Lett. 24 (1994) 107.
[6] J.P. Cuif, G. Blanchard, O. Touret, A. Seigneurin, M. Marczi, E. Quémeré, SAE publication no. 961906 (1996).
[7] H. Vidal, J. Kašpar, M. Pijolat, G. Colon, S. Bernal, A.M. Cordon, V. Perrichon, F. Fally, Appl. Catal. B: Environ. 27 (2000) 49.
[8] G. Colon, M. Pijolat, F. Valdivieso, H. Vidal, J. Kašpar, E. Finocchio, M. Daturi, C. Binet, J.C. Lavalley, R.T. Baker, S. Bernal, J. Chem. Soc., Faraday Trans. 94 (1998) 3717.
[9] H.C. Yao, Y.F. Yu Yao, J. Catal. 86 (1984) 254.
[10] P. Fornasiero, G. Balducci, R. Di Monte, J. Kašpar, V. Sergo, G. Gubitosa, A. Ferrero, M. Graziani, J. Catal. 164 (1996) 173.
[11] V. Perrichon, A. Laachir, S. Abouarnadasse, O. Touret, G. Blanchard, Appl. Catal. A: Gen. 129 (1995) 69.
[12] F. Fally, V. Perrichon, H. Vidal, J. Kaspar, G. Blanco, J.M. Pintado, S. Bernal, G. Colon, M. Daturi, J.C. Lavalley, Catal. Today 59 (2000) 373.
[13] V.G. Keramidas, W.B. White, J. Am. Ceram. Soc. 57 (1974) 22.
[14] T. Egami, W. Dmowski, R. Brezny, SAE publication no. 970461 (1997).